Observation of the Quantum-Confined Stark Effect in a GaAs/AlGaAs P-I-N Diode by Room Temperature Photocurrent Spectroscopy

C.S. Ison*, E.S. Estacio, M.F. Bailon, and A.A. Salvador

Condensed Matter Physics Laboratory, National Institute of Physics
College of Science, University of the Philippines Diliman
1101 Quezon City, Philippines
E-mail: cison@nip.upd.edu.ph

ABSTRACT

Room temperature photocurrent spectroscopy is performed on an MBE-grown GaAs/AlGaAs MQW p-i-n device. An observed shift to longer wavelengths is seen with increasing reverse bias voltages. This behavior is explained through a mechanism called the Quantum-Confined Stark Effect. Applied electric fields are estimated using second-order correction for infinite quantum wells. The estimated built-in electric field is 20 kV/cm corresponding to a 9-meV shift from the flatband energy transition. An observed shift to shorter wavelengths is seen under an optically applied field for both biased and unbiased conditions.

INTRODUCTION

GaAs-based devices have recently found widespread use in modern telecommunications. Being a direct band-gap semiconductor, GaAs boasts of efficient and fast carrier recombination rates (Sze, 1969). The incorporation of an undoped multiple quantum well (MQW) region between the conventional p-n junction has allowed for the further improvement of the absorption and transit time of carriers. In addition, the absorption of these p-i-n devices peaks abruptly at the energy levels of the MQW. Thus, the region of operation of a p-i-n device may be specified by appropriately choosing the well width of the active MQW region (Singh, 1993). This property of quantum well-based devices provides many important and useful benefits and effects for optoelectronic applications.

The application of an electric field perpendicular to the plane of the QW influences its properties. Among the prominent effects observed is the Quantum-Confined Stark Effect (QCSE). At flat band condition (zero-field), a QW is simply treated as a quantum mechanical "particle-in-a-box", wherein the electron and hole have symmetric sinusoidal wavefunctions from which the energy of inter-subband transitions for the excitons (e-h pairs) can be easily obtained. With electric field, band bending occurs, forming a tilted-quantum well, which results in the lowering of energy band transitions, i.e., the electron subband energy level drops and the hole subband energy level rises. Also the excitons are "polarized" since the wavefunctions of the electrons and holes are pulled towards opposite directions, as illustrated in Fig. 1. As an effect, the band edge absorption is quadratically reduced, broadened, and shifted to lower energy (Loehr, 1996; Klingshirn, 1997.).

Photocurrent (PC) spectra are considered to imitate the photoabsorption spectral lineshape, when the photo-generated carriers escape the MQW active region and cross the heterojunction. This involves photoabsorption
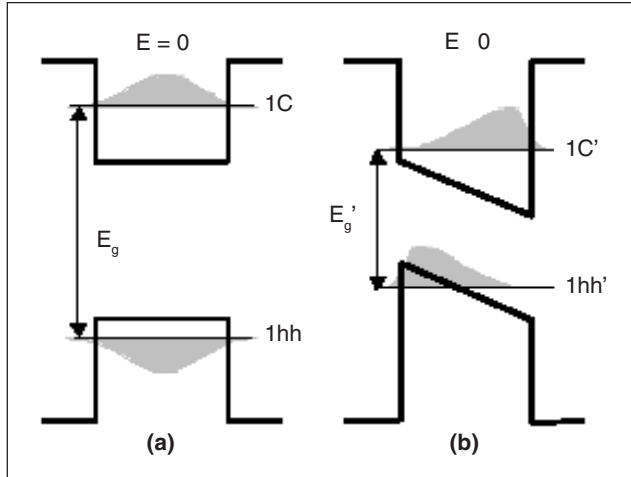
* Corresponding author

Fig. 1. The band structure of a quantum well (a) without and (b) with an applied electric field perpendicular to the wells. The interband transition energy decreases as greater field strength is applied.

and transport of photo-carriers across the junction yielding the photocurrent (Kawasaki et al., 1999). As direct absorption experiments in devices require intricate substrate-etching sample preparations, PC spectroscopy offers the best alternative in studying the band structure of an MQW active region incorporated in a p-i-n structure.

This band-gap tailoring capability, together with the exploitation of the QCSE, has led to novel devices, such as optically bistable self-electrooptic effect devices (SEED)(Miller et al., 1986; Lentine & Miller, 1993). The authors present results on the observation of the QCSE in the MQW active region of an MBE-grown p-i-n diode. Room temperature photocurrent spectroscopy was performed with reverse bias voltage and an optically applied forward bias.

EXPERIMENTAL METHOD

The sample used was grown on an n-type GaAs (100) substrate by molecular beam epitaxy. The designed quantum structure consists of 3 periods of 90 Å GaAs quantum wells and 100 Å AlGaAs barriers. This undoped quantum structure is confined by undoped 100 Å $Al_{0.3}Ga_{0.7}As$ layers. These layers contained in the intrinsic region are sandwiched by n- and p-$Al_{0.3}Ga_{0.7}As$ cladding layers to form a p-i-n structure. Ohmic indium

contacts were soldered on a 1.5 mm^2 piece of the MBE-grown p-i-n structure. Fig. 2 shows the current-voltage characteristics of the device. The breakdown voltage is estimated to be 2.0 V.

Room temperature PC measurements were done using the same experimental setup utilized by Ison et al. (2000). The spectra were probed by light from a 100 W Tungsten-Halogen lamp dispersed by a SPEX 500M monochromator. The probe beam is mechanically chopped at 200 Hz and focused into the sample by suitable optics. The photo-induced current was then fed to an SR510 lock-in amplifier using the chopping frequency as reference. System control and data acquisitions were done by computer. PC spectra were acquired for no reverse bias, 0.5 V, and 1 V reverse bias. In addition, an optically applied forward bias (using an Ar^+ laser) was employed to counteract band bending due to QCSE.

RESULTS AND DISCUSSION

The flat band energy transitions for the excitons were measured via photoluminescence (PL) of a different multiple quantum well sample. The PL peaks provide the excitonic transitions (1HH-1C and 1LH-1C) for a 90 Å GaAs/AlGaAs quantum well. These peaks were verified using the effective mass approximation method
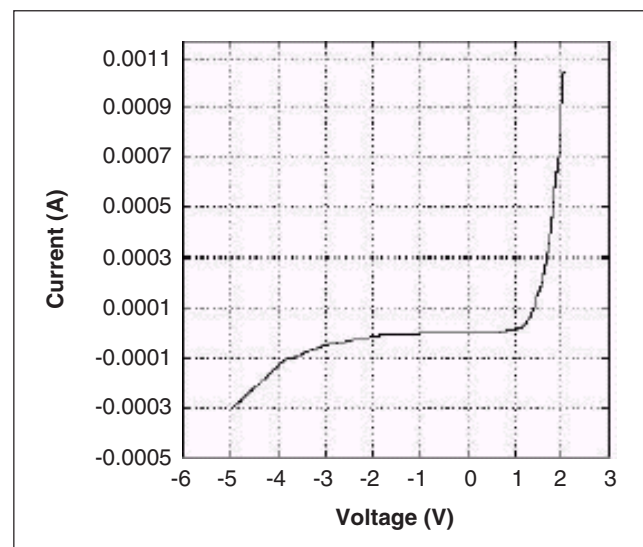

Fig. 2. Current-voltage characteristics of the p-i-n structure. The estimated breakdown voltage is 2.0 V.

(Chang, 1996). The energy position for the first light hole transition (1LH-1C) occurs at 8430 Å (1.471 eV) while the first heavy-hole transition (1HH-1C) occurs at 8480 Å (1.462 eV). Comparing the flat band energy locations of the allowed transitions (PL peaks) with the features observed in the zero-bias PC spectrum in Fig. 3, the excitonic energy levels are shifted toward longer wavelengths (red-shift). For the PC spectra, the energy position for the 1LH-1C transition occurs at 8423 Å (1.470 eV) while the 1HH-1C transition occurs at 8531 Å (1.453 eV). This red shift corresponds to a calculated 20 kV/cm built-in field. The shifting of the excitonic transitions toward lower energies is an evidence of QCSE.

Eq. (1) gives the energy level of a zero-field infinite quantum well.

$$E_n = \frac{n^2 \pi^2 h^2}{2m^* L^2}; \quad n = 1, 2, 3, \ldots \tag{1}$$

Using a second order correction for the infinite quantum well, Bastard et al. obtained the relationship of the field (F) with the change in the energy level, as given by Eq. (2),

$$\Delta E_1 = -\frac{|e|FL}{2} + \left(\frac{3}{2}\right)^{\frac{5}{3}} \left(\frac{e^2 h^2 F^2}{m^*}\right)^{\frac{1}{3}} \tag{2}$$

where F is the electric field strength, m^* is the effective mass, and L is the width of the quantum well.

The other features at lower wavelengths correspond to Fabry-Perot oscillations resulting from the abrupt interface between the MQW and the cladding region (Lacap et al., 2000). These equally spaced modes are generally unaffected by the application of an electric field.

To investigate further the effects of electric fields on the QW in a p-i-n structure, PC measurements were done at different reverse bias voltages. Fig. 4 shows the PC spectra under an applied voltage of -0.5 V and -1.0 V. Under reverse bias, the additional electric field causes the tilting of the quantum wells to increase. The observed energy shifts due to band tilting were used to estimate the electric field strengths in the *i* region. These shifts were taken relative to the flatband condition.
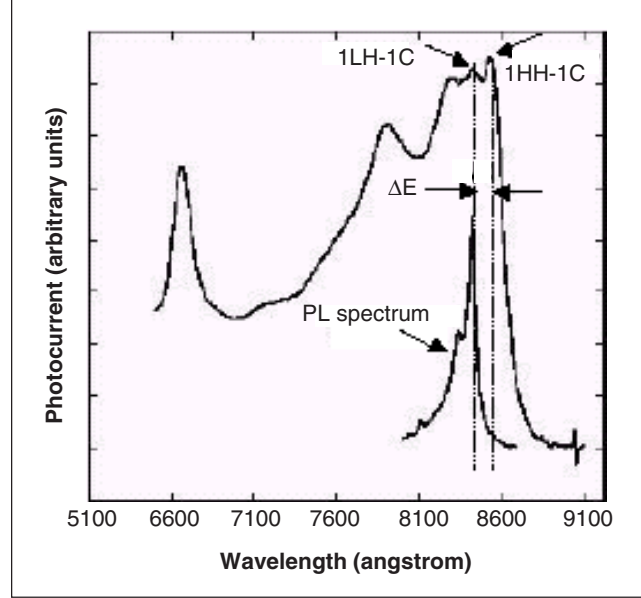

Fig. 3. PL spectra showing the 1HH-1C and 1LH-1C excitonic spectra under flat band conditions and the PC spectra at zero bias.
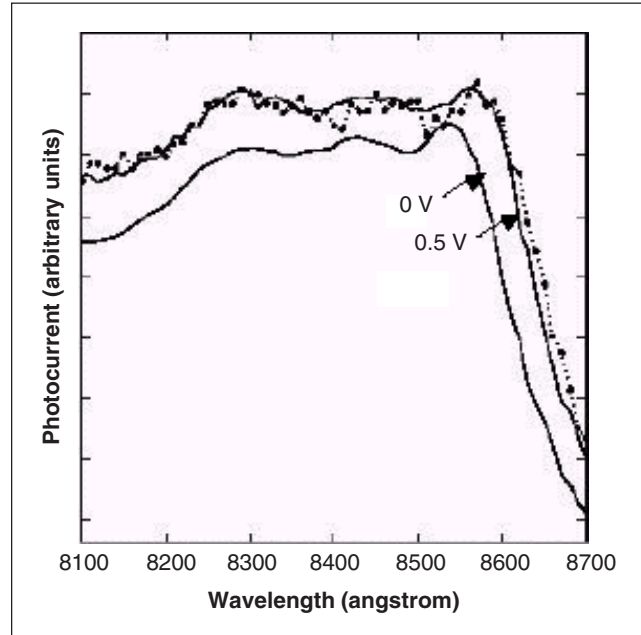

Fig. 4. PC spectra at zero bias, 0.5 V, and 1 V reverse bias showing shifts to higher wavelengths with increasing reverse bias voltages. The dotted spectrum corresponds to 1 V reverse bias.

Table 1 shows the excitonic transitions with their corresponding applied electric field strengths. The first order approximation of the electric field strength uses

Table 1. Excitonic transition energies with estimated electric field calculated from observed energy shifts.

	Field (kV/cm)		Transition energies (eV)		Energy shift relative to flatband (meV)	
	1st Order	2nd Order	1HH-1C	1LH-1C	1HH-1C	1LH-1C
Flatband	0.0	0.00	1.462	1.471		
Unbiased	20.0	20.03	1.453	1.470	9	1
0.5 V reverse bias	31.1	31.15	1.448	1.468	14	3
1.0 V reverse bias	37.8	37.85	1.445	1.465	17	6

parallel-plate capacitor calculations. The second order correction terms for the infinite quantum well assumption were also taken into account, but did not introduce any significant deviation from the first order approximation. As expected, the increase in the applied field results in longer transition wavelengths (lower energies). It is also apparent in Fig. 4 that the intensity of the PC spectra increases for biased samples. This can be explained by the distortion of the electron and hole wavefunctions, wherein an applied field decreases the exciton binding energy, causing an increase in the tunneling efficiency (Haug, 1988). As a further note, the "smoothing" of the PC spectra at 1.0 V reversed bias compared to the 0.5 V spectra is a direct consequence of the relaxation of the allowed transitions (band edge) and filling up of the forbidden transitions (lower wavelengths). The electric field essentially does not increase the amount of absorption (Miller et al., 1985).

The sample was also subjected to an optically applied field, effectively forward biasing the p-i-n junction. This was done by illuminating the sample with an Ar^+ laser (488 nm). Fig. 5 shows the PC spectra under an optically applied field. The estimated incident photon flux is in the order of 1,015 photons/second with an input power of 2 mW. The number of electronhole pairs was determined from the estimated fields; each is in the order of $1,010/cm^2$. The comparatively lower number of calculated electron-hole pairs is attributed to many factors, among which is the difference in tunneling probabilities of the AlGaAs barriers and the GaAs wells, GaAs being slightly p-type (unintentionally doped), and due to reflection of the incident photons, by the thick n-type and p-type layers. An observed blue shift to shorter wavelengths is seen for both no bias and reverse biased conditions, with no significant increase in PC intensity. The blue shift in the no bias condition closely approximates the flatband transition seen in PL spectra in Fig. 2. Illumination of the sample under 0.5 V reverse bias causes the shifted excitonic peaks to revert back to the excitonic peak positions of the unbiased state because the field created by the laser counteracts the field caused by the applied bias.

SUMMARY OF RESULTS

Room temperature PC spectroscopy was performed on an MBE-grown GaAs/AlGaAs MQW p-i-n device. An observed shift to longer wavelengths is seen with increasing reverse bias voltages characteristic of the Quantum-Confined Stark Effect. Applied electric fields were estimated using second-order correction for
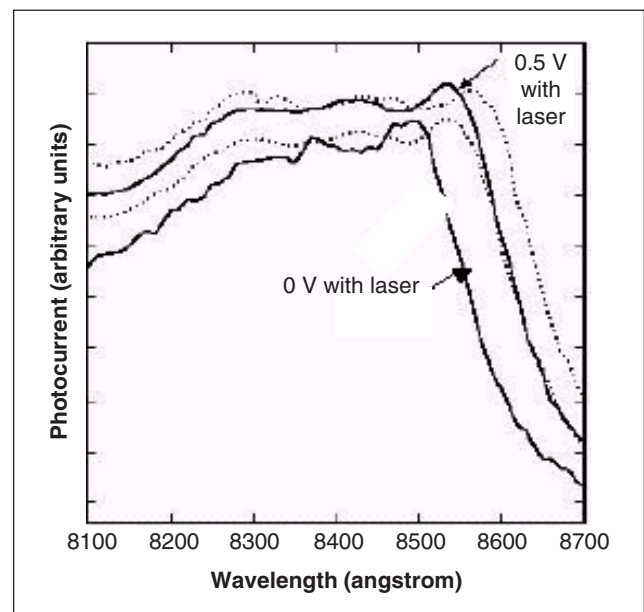

Fig. 5. PC spectra under an optically applied field for zero bias and 0.5 V reverse bias. Dotted lines correspond to PC spectra without illumination.

Table 2. Summary of transition energies as a function of applied electric and optical fields.

| | Estimated Field (kV/cm) | Transition energies (eV) | | | |
| | | without applied optical field | | with applied optical field | |
		1HH-1C	1LH-1C	1HH-1C	1LH-1C
Flatband	0.0	1.462	1.471	---	---
Unbiased	20.0	1.453	1.470	1.460	1.482
0.5 V reverse bias	31.1	1.448	1.468	1.453	1.472
1.0 V reverse bias	37.8	1.445	1.465	---	---

infinite quantum wells. Table 2 gives a summary of the calculated electric field strengths and transition energy shifts under applied electric and optical fields. The estimated built-in electric field is 20 kV/cm corresponding to a 9-meV shift from the flatband transition.

An observed blue shift is seen under an applied optical field for both biased and unbiased conditions, reverting the tilted band edge to a nearly "flatband" condition.

ACKNOWLEDGMENT

REFERENCES

Chang, Y., 1996. Band structures of III-V quantum wells and superlattices. In Bhattacharya, P. (ed.) Properties of III-V quantum wells and superlattices. *INSPEC*. 35-41.

Haug, H., 1988. Optical nonlinearities and instabilities in semiconductors. New York, Academic Press.

Ison, C., E. Estacio, J. Laniog, & A. Salvador, 2000. Time-resolved photocurrent spectroscopy of an LPE-grown GaAs/AlGaAs heterojunction device. *Proc. 18th SPP Physics Congress*. 85-87.

Kawasaki, K., et.al., 1999. Interplay of excitonic radiative recombination and ionization in photocurrent spectra of thick barrier GaAs/AlAs multiple quantum wells. *Jpn. J. Appl. Phys*. 38: 2552-2554.

Klingshirn, C.F., 1997. Semiconductor optics. Berlin Heiddelberg, Springer-Verlag. 259-263.

Lacap, N., E. Estacio, A. Podpod, & A. Salvador, 2000. Photocurrent spectroscopy of a resonant cavity enhanced photodetector. *Proc. 18th SPP Physics Congress*. 76-78.

Lentine, A.L. & D.A.B. Miller, 1993. Evolution of the SEED technology: Bistable logic gates to optoelectronic smart pixels. IEEE. *J. Quant. Electr*. 29(2): 655-669.

Loehr, J.P., 1996. Effects of electric fields in quantum wells and superlattices. In Bhattacharya, P. (ed.) Properties of III-V quantum wells and superlattices. *INSPEC*. 71-73.

Miller, D.A.B., J.S. Weiner, & D.S. Chemla, 1986. Electric-field dependence of linear optical properties in quantum well structures: Waveguide, electroabsorption, and sum rules. IEEE. *J. Quant. Electr*. QE-22(9): 1816-1830.

Miller, D.A.B., D.S. Chemla, T.C. Damen, A.C. Gosard, W. Wiegmann, T.H. Wood, & C.A Burrus, 1985. Electric field dependence of optical absorption near the band-gap of quantum well structures. *Phys. Rev. B*. 32(2): 1043.

Singh, J., 1993. Physics of semiconductors and their heterostructures.

Sze, S.M., 1969. Physics of semiconductor devices. John Wiley and Sons. 57.